

Article

# Implementing Digital Edge Enhancers on Improved High-Resolution Aeromagnetic Signals for Structural-Depth Analysis around the Middle Benue Trough, Nigeria

Eko Gerald Ejiga \*, Noer El Hidayah Ismail \* and Ismail Yusoff

Department of Geology, Faculty of Science, University of Malaya, Kuala Lumpur 50603, Malaysia; ismaily70@um.edu.my

\* Correspondence: sva170050@siswa.um.edu.my (E.G.E.); noerelhidayah@um.edu.my (N.E.H.I.)

**Abstract:** Digital edge detector operations using magnetic derivatives in conjunction with spectral depth analysis were performed on high-resolution aeromagnetic signals to enhance the delineation and interpretation of depth, structural, and intrasedimentary features within the Middle Benue Trough (MBT) of North Central Nigeria, which could serve as a guide for mineral exploration. The derivatives revealed high-amplitude and short-wavelength anomalies over areas underlain by crystalline basement complexes, major volcanic zones, and aggregates of intrasedimentary volcanic and plutonic rocks. Geologic lineaments trending predominantly NE–SW and NW–SE, as well as minor trends of E–W and N–S, suggest that the area has undergone differential stress regimes across geologic time. The spectral depth analysis indicates a two-source depth model. The deep depth ranges from 1.9 to 6.1 km with an average of 3.9 km, whereas the shallow depth ranges between 0.3 and 1.9 km with an average of 0.8 km and is found to emanate from magnetic signals of post-Cretaceous near-surface igneous intrusions as well as other magnetized bodies embedded within the sediments. The spatial distribution of various hydrothermal minerals such as lead–zinc–barite deposits, as well as salt mineralization, is associated with the widespread Tertiary–recent magmatism and governed by pre-existing tectonic structures in the region.

**Keywords:** magnetic derivative; spectral depth analysis; Middle Benue Trough; intrusive; hydrothermal minerals; edge detector



check for updates

**Citation:** Ejiga, E.G.; Ismail, N.E.H.; Yusoff, I. Implementing Digital Edge Enhancers on Improved High-Resolution Aeromagnetic Signals for Structural-Depth Analysis around the Middle Benue Trough, Nigeria. *Minerals* **2021**, *11*, 1247. <https://doi.org/10.3390/min1111247>

Academic Editor: Stanisław Mazur

Received: 27 September 2021

Accepted: 6 November 2021

Published: 10 November 2021

**Publisher's Note:** MDPI stays neutral with regard to jurisdictional claims in published maps and institutional affiliations.



**Copyright:** © 2021 by the authors. Licensee MDPI, Basel, Switzerland. This article is an open access article distributed under the terms and conditions of the Creative Commons Attribution (CC BY) license (<https://creativecommons.org/licenses/by/4.0/>).

## 1. Introduction

The potential field methods of geophysical surveying involving the aeromagnetic exploration technique have proven to be reliable and cost-effective in mapping large areas over a short time. Of particular significance is its usefulness in determining a region's structural framework, magnetic source depths, geotectonics, geothermal potentials, and various reconnaissance explorational activities. It is also helpful for identifying intrasedimentary features, volcanic rocks, or igneous intrusions that may disrupt a region's typical sedimentary pattern [1]. Mapping the source locations that generate the anomalies is an important step in the structural-depth analysis of potential field data because the source edges can be used in a variety of applications, including mineral and petroleum exploration [2,3]. The lateral boundaries of source bodies play a critical role in interpreting and constraining depth models and structural frameworks, both of which are important in understanding the geology of an area. Edge detection involves the use of filters to distinguish points on a gridded dataset where physical properties such as magnetization contrast or discontinuities are encountered. These points are structured into a series of linear fragments known as edges. Several techniques have been developed to enhance the delineation of edges of source bodies using gravity and magnetic data [4–10].

The derivatives of potential field data can be described as the rate of change of anomaly or magnetic intensity values in different directions of the geomagnetic field. They

act as magnetic vectors that provide extra information regarding the total magnetic field's directional variation [11,12], and help in defining/estimating the physical properties of the source structure generating the anomaly [7]. Magnetic derivatives-based operations are effective in enhancement of magnetic anomalies, thus making it easier for detecting geologic body edges as well as structural mapping and delineating intrasedimentary intrusions. They are also useful in locating surface and subsurface faults, shear zones, and fractures [4,7]. Some of these structures could be used as guides to areas of epigenetic, stress-related, hydrothermal mineralization [13,14]. The edge detectors techniques use magnetic derivatives to emphasize edges of magnetization boundaries, and the most commonly applied are the vertical and horizontal derivatives [15,16]. However, the limitation to the vertical and horizontal derivatives is that determination of diminishing anomalies is often burdensome and ambiguous due to high-amplitude variations of signals emanating from sources of contrasting depths, geometries, and magnetization properties [7,17]. To overcome this limitation, other enhancement techniques, such as the tilt derivative and the analytic signal, as well as the upward and downward continuation filters, can also be applied in order to resolve complex anomalies.

Depth estimations through quantitative analysis of magnetic anomalies have become common and can be performed both in space and frequency domains. In frequency/wavenumber domain, however, depth estimation to magnetic sources is easier and more convenient since the convolution operator is easily converted to multiplication notation through Fourier transform [18,19]. Hence, since the 1970s, the interpretation of aeromagnetic data using the Spector and Grant [20] technique has become very popular and important for the estimations of depth to the top of magnetic sources. This method, in which the top depth is simply related to the magnetic field's power spectrum, can also be used to estimate the depth of various subsurface geological features and basement relief [21–23]. Because most mineralization occurs in areas with widespread magmatism and tectonism, delineation of depth, structural, and intrasedimentary features can help to improve knowledge of the spatial distribution of various hydrothermal minerals such as salt (NaCl) and barite (BaSO<sub>4</sub>) in the trough. This study is aimed at interpreting and better understanding the Middle Benue Trough's (MBT) structural framework and depth geometries, as well as the influence of the widespread volcanism and plutonism on hydrothermal mineralization, which ultimately will benefit future exploration for solid minerals and hydrocarbon in the area.

## 2. Geologic Setting

The Benue Trough of Nigeria is a long, elongated rift system that runs roughly NE–SW for about 800 km in length and 150 km in width. Due to its hydrocarbon and other economic mineral potentials, such as coal, lead, zinc, copper, silver, barites, fluorspar, gypsum, limestones, and anhydrite [24], it is considered a rift of great economic significance in Nigeria's geology. The trough formed during the Late Jurassic to Early Cretaceous, through a faulted rift system that opened the South Atlantic Ocean and the Gulf of Guinea, consequently leading to the separation of Africa from South America [25–29]. The Rift–Rift–Fail (RRF) triple junction system, which includes the South Atlantic shore, the Gulf of Guinea, and the Benue Trough, was formed as a result of that tectonic event. The Benue Trough is thought to be the triple junction's failed arm [25,27]. Grant [30] suggested that the Niger Delta was the location of the RRF triple junction, with the Benue Trough serving as the tensile “F-arm” that partially closed after South America and Africa were separated. The Albian marine invasion, accompanied by compressive folding of the accumulated sediments in the Santonian, followed by “rebound” due to strain accumulation in the African plate invariably account for these tectonic events [30,31]. The Lower Benue Trough (LBT), Middle Benue Trough (MBT), and Upper Benue Trough (UBT) are the three tectonic sub-troughs comprising the Benue Trough [26]. Figure 1 shows the tectonic map of the West and Central African Rift System and the location of the MBT.

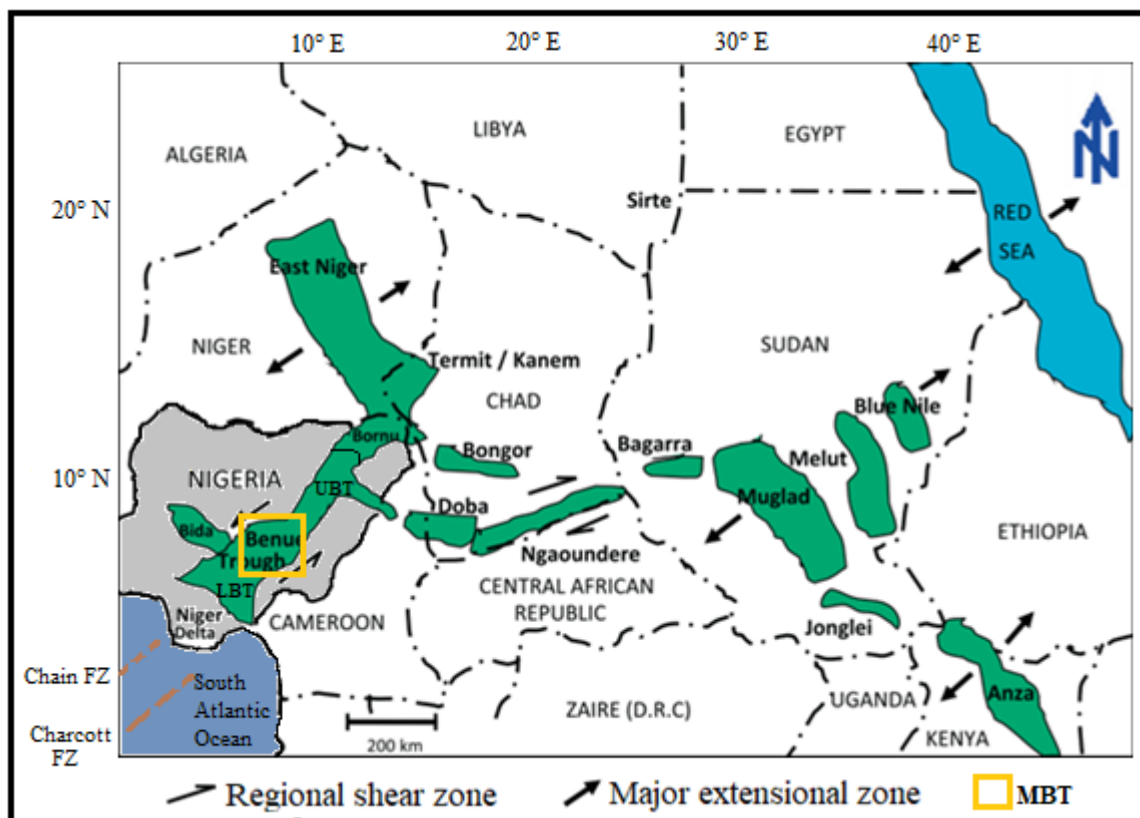


**Figure 1.** West and Central African Rift System regional tectonic map. FZ denotes fracture zone (modified after Schull [32] and Anudu et al. [1]).

The study region is situated in the MBT in North Central Nigeria, between latitude  $7^{\circ}$  to  $9^{\circ}$  N and longitude  $8^{\circ}$  to  $10^{\circ}$  E. The MBT, which connects the Lower and the Upper Benue Trough (LBT and UBT), is made up of the Basement Complex rock units, younger granites, sedimentary basins, and Tertiary–recent volcanics (Figure 2). The Precambrian Basement Complex rocks, however, are the oldest rock units in the area, remobilized and uplifted relative to the surrounding rocks during the Pan-African orogeny (600–500 Ma). These Basement Complex rocks include the Migmatite Gneiss Complex, schist, and Older Granite, and are found primarily in the extreme northern and southern portions of the basin, largely enclosing the MBT as well as outcropping within the central areas of the basin. The Migmatite Gneiss Complex found within the study area comprises rocks of migmatite, which outcrop predominantly in the northeastern portion around Kwafide; the migmatite gneiss in the southeastern parts around towns such as Amadu and Katsina-Ala, as well as around Wamba environs in the northwest; the granite gneiss which outcrops mainly around Wamba in the northwestern part, and the Older Granites which are found in a number of locations, including Gboko in the south, around Zaki Biam in the central portion, and areas around Lafia and Garaku in the northwestern zones. The presence of some undifferentiated granites, migmatites, granite gneisses, and Older Granites can, however, be found in the northernmost zone of Garaku. The migmatite gneiss in these areas is composed of migmatite gneisses and porphyroblastic gneisses. Biotite and banded gneisses dominate the granite gneisses of that area, while the Older Granites are predominantly medium- to coarse-grained biotite granites. The Basement Complex was intruded by the Younger Granites ring complexes in the northwestern portion around Wamba, Baminga, and north of Lafia. The rock types that make up the Younger Granites in the area are mostly biotite granite, which occurs primarily in distinct annular cone sheets, as opposed to the porphyry ring dykes that characterize the majority of Nigeria’s Younger Granite ring complexes.

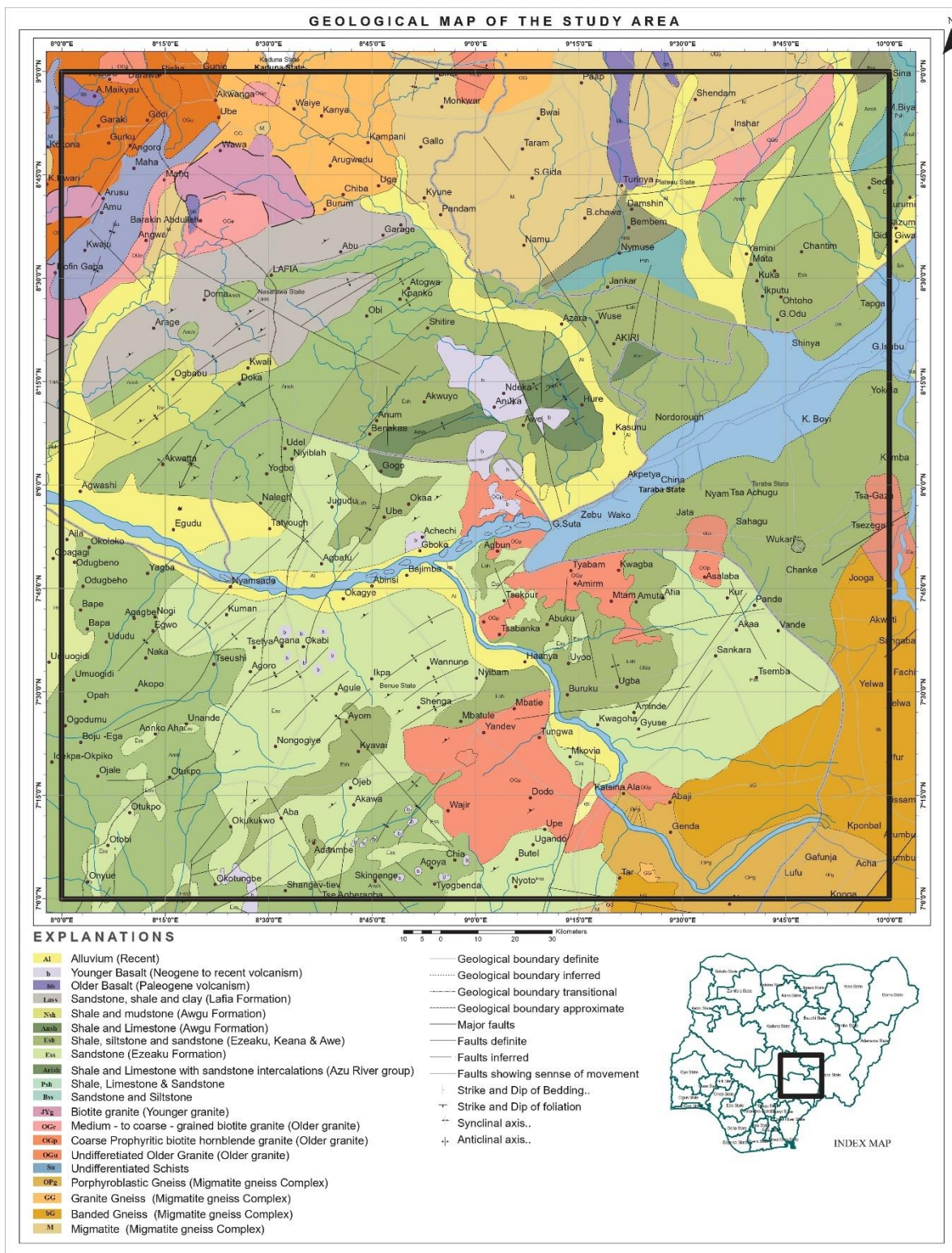


**Figure 2.** Geological map of the study area (modified after Nigeria Geological Survey Agency [33]). Inset is an index map showing the study area’s location within Nigeria’s landmass.

Detailed stratigraphic discussions of the sedimentary formations within the Middle Benue Trough were provided by [24,26,34,35]. The succession is composed of the Asu River Group of sediments, which are considered as the earliest sedimentary deposits in the region, and consist of marine-derived sediments that represent the first Albian transgression into

the Benue Trough [34,35]. The Asu River Formation is overlain by transitional beds of the Awe Formation, which mark the start of the regressive phase of the Albian Sea. The Keana Formation, composed of continental sediments, overlies the Awe Formation. The Ezeaku Formation comes next, followed by the Awgu Formation, and, finally, the Lafia Formation, all representing the Turonian to Maestrichtian sediments comprising primarily sandstones, siltstones, and limestones [24,26,34,35]. Volcanic rocks in the area date from the Tertiary–recent period and are found in abundance.

### 3. Materials and Methods

#### 3.1. Acquisition of the High-Resolution Aeromagnetic Data (HRAD)

The first airborne magnetic surveys in Nigeria were performed in the 1970s. The survey data were collected at 2 km flight line spacing, terrain clearance/flight elevation of 150 m, and tie line spacing of 20 km, and were only available in analogue paper format in the archives. These old surveys have no doubt played an important role in understanding the country's regional geology, but their analogue nature and low resolution have limited their utility. As a result, there was a need to upgrade and update this old 1970s data by generating a new high-resolution aeromagnetic map that will bring out more detailed features to assist in understanding the country's geology more thoroughly. Therefore, an enormous country-wide airborne geophysical survey involving data acquisition, preliminary processing, and storage began in 2003 and lasted until about 2009. It accumulated thousands of flight hours. The survey was conducted by Fugro Airborne Surveys and was performed in two phases. Phase 1 was concluded in September 2007 with 826,000 line-km of magnetic and radiometric surveys flown at 500 m flight line spacing and 80 m terrain clearance, and was wholly funded by the Nigerian Government [36]. Phase 2 was completed in August 2009, with parts of the funding coming from the World Bank, under a larger project known as the Sustainable Management for Mineral Resources Project. It included 1,104,000 line-km of magnetic and radiometric surveys flown at 500 m line spacing and 80 m terrain clearance to survey areas that were not covered in Phase 1 [36]. These surveys are intensive because seven aircraft of three different types were active almost every time the investigation was conducted [36]. The data were subjected to all necessary magnetic corrections, including the diurnal variations and the international geomagnetic reference field (IGRF), using the 2005 model, before being stored at the NGS office. Figure 3 depicts data acquisition techniques in illustrative form.

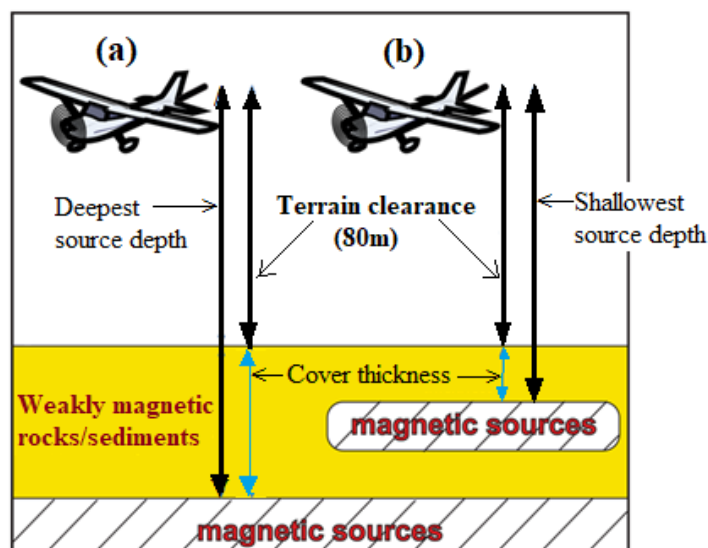


**Figure 3.** An illustration of the data acquisition for the high-resolution aeromagnetic data (HRAD), showing the depths to the top of (a) deepest magnetic sources and (b) shallowest magnetic sources.

### 3.2. Edge Detector Operations

The vertical derivative using the fast Fourier transform (FFT) enhances the shallower geologic features in an area by amplifying the high-frequency/short-wavelength component of the data, while at the same time suppressing the low-frequency/long-wavelength component which arises from the deep regional field [37]. These operations can be performed either by using the first vertical derivative (VDR/1VD), the second vertical derivative (2VD), or even higher orders of vertical derivatives. However, higher orders of more than two are practically never used to generate interpretable results, as the noise in the data becomes more amplified than the signal above the order of two. Zero contours of the 1VD or the 2VD may be used to outline the approximate boundaries of magnetic sources as it is often inferred to correspond to geological boundaries [38]. The mathematical expression for the first vertical derivative is given as

$$1VD = \frac{\partial M}{\partial z} \quad (1)$$

While the second vertical derivative can be expressed as

$$2VD = \frac{\partial^2 M}{\partial z^2} \quad (2)$$

The total horizontal derivative (THDR) enhances the anomaly texture, pattern, and discontinuities, thereby making the edges of the causative sources accentuated and clearer. It usually peaks over magnetic contacts on the assumption that the regional magnetic field and the source magnetization are vertical [39]. As a result, the ridges or maxima of the horizontal derivatives are good locators of the edges of magnetic bodies. A major advantage of THDR over other derivatives is that it is less sensitive to noise and is effective in delineating both shallow and deeper magnetic sources [39]. The relationship can be expressed as [4]

$$THDR = \sqrt{\left(\frac{\partial M}{\partial x}\right)^2 + \left(\frac{\partial M}{\partial y}\right)^2} \quad (3)$$

where  $\frac{\partial M}{\partial x}$  and  $\frac{\partial M}{\partial y}$  are derivatives in x and y direction of the magnetic field M.

The tilt derivative (TDR) was introduced by Miller and Singh [5] for normalizing different amplitudes emanating from different magnetic sources of contrasting depth. In this operation, the amplitude of the VDR is normalized by its THDR. Its function is expressed mathematically as [5,7]

$$TDR = \tan^{-1} \left( \frac{VDR}{THDR} \right) = \tan^{-1} \left[ \frac{\frac{\partial M}{\partial z}}{\sqrt{\left(\frac{\partial M}{\partial x}\right)^2 + \left(\frac{\partial M}{\partial y}\right)^2}} \right] \quad (4)$$

The amplitude variation of the tilt angle has a specific range between  $-\pi/2$  to  $\pi/2$ , similar to an automatic gain control (AGC) filter that magnifies the amplitude of low-level signals at different depths, as well as equalizing responses emanating from both strong and weak anomalies [7]. The TDR has three rates of amplitude: positive over the source, zero at/near the edge of the source, and negative outside the source. However, its zero contours correspond to source edges, which often correlate to geologic discontinuities that can be utilized to trace linear structures [5,15]. This function is very effective in the presence of noise and good at detecting sources of both shallow and intermediate depths. While other conventional derivatives exhibit amplitudes that resemble the total magnetic intensity (TMI) anomaly, the TDR, on the other hand, is independent of the TMI amplitude and is governed by the reciprocal of the source depths [7].

The analytic signal (AS) amplitude of a TMI, as proposed by Roest et al. [6], is commonly utilized in magnetic interpretation to position anomalies directly over their causative

sources. This approach is most useful at low magnetic latitudes, due to the significant distortion of anomalies caused by low-latitude pole reduction operations [6,40]. It tends to display maxima over magnetization contrasts; therefore, location of these maxima thus determines the outlines and geometry of the magnetic source as well as locations of faults, joints, lithological contacts, shear zones, volcanic plugs, dykes, and isolated bodies. While Nabighian [41] developed the 2D AS for profile data, Roest et al. [6] demonstrated that the absolute value of the 3D AS can be determined by the square root of the squared sum of derivatives in the three orthogonal directions (x, y, and z) of the magnetic field as

$$|AS(x, y)| = \sqrt{\left(\frac{\partial M}{\partial x}\right)^2 + \left(\frac{\partial M}{\partial y}\right)^2 + \left(\frac{\partial M}{\partial z}\right)^2} \quad (5)$$

where  $|AS(x, y)|$  is the amplitude of the AS at x, y, and  $\frac{\partial M}{\partial x}$ ,  $\frac{\partial M}{\partial y}$ , and  $\frac{\partial M}{\partial z}$  are derivatives in x, y, and z directions of the magnetic field, M.

Although the amplitude of the 2D AS is independent of both the ambient field and the direction of source magnetization, the 3D case, on the other hand, is dependent on all the Earth's magnetic field parameters, including the direction of the inducing magnetic field, remanent magnetization direction, the dip, and depth of the source body [42]. Nonetheless, the 3D AS is effective for edge detection and may complement the THDR technique, as well as resolve the complex problems of low magnetic latitudes, particularly those with geomagnetic inclination less than  $20^\circ$ , where the application of the reduction to the pole (RTP) results in uninterpretable anomalies [8,40,42]. The magnetic field's geometrical relationships between the various derivatives computed for this study are described in Figure 4.

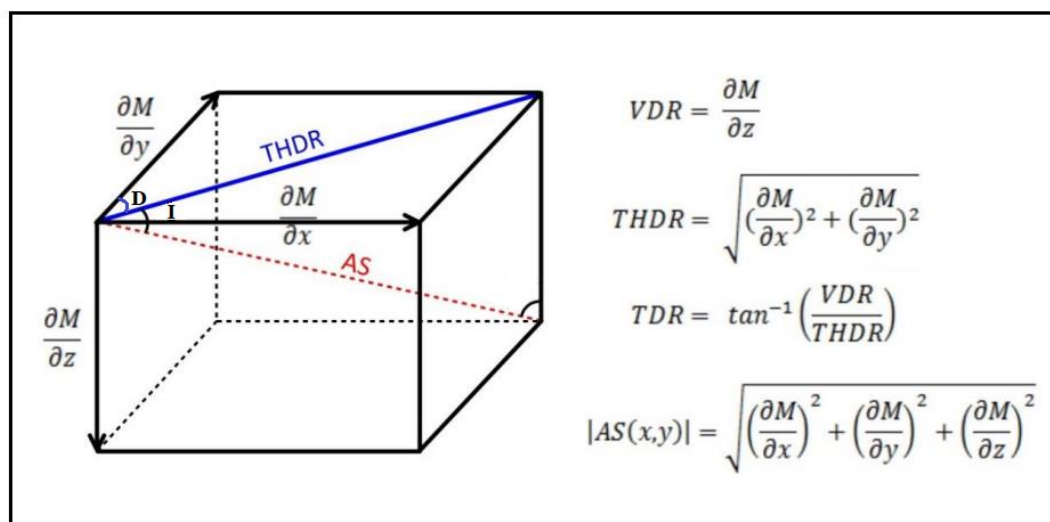


**Figure 4.** Definition of the geometrical relationships between VDR, THDR, TDR, and AS. D and I represent the angles of declination and inclination, respectively [17].

### 3.3. Spectral Depth Analysis

The Earth's magnetic field can be used to find the depth of anomalous sources which can be as shallow as a few meters to tens of kilometers through spectral analysis method. This method involves analyzing or interpreting aeromagnetic data using either 1- or 2-dimensional spectral analysis comprising different frequencies in which the anomalies are characterized. By radial averaging, a 2D power spectrum can be converted to a 1D spectrum, which relates to the frequency/wavenumber's amplitude, thereby constituting the complex line spectrum from which depths estimation can be derived. In applying this technique, the Earth is assumed to be an assemblage of rectangular and vertical-sided

parallelepipeds whose depth width, thickness, and magnetization intensity are variable [20]. The calculated average spectrum of anomalies within a given frequency range represents the radial spectrum of the anomalous field [20,43,44]. The mean ensemble depth,  $d$ , is equivalent to half the slope on the logarithmic radial spectra. If there are two sets of magnetic sources, then they can be recognized by remarkable changes in the spectra decay rate. Hence, the power spectrum of the double ensemble will consist of two parts. The first part, which relates to the deeper magnetic sources, is relatively strong at lower frequencies and decays away rapidly. The second, which arises from a shallower ensemble of magnetic sources, dominates the high-frequency end of the spectrum. This statistical method of depth calculations has been proven to yield good estimates to the top of magnetic sources and have been applied by various authors [20,22,43–45].

Taking  $d$  to be the mean depth of the layer, the depth factor for this magnetic ensemble of anomalies can be expressed as exponent  $(-2dk)$ . Thus, the logarithmic plot of the radial spectrum against the frequency/wavenumber gives a straight line having a slope of  $-2d$ . Therefore, the ensemble's average depth can be obtained from

$$d = \frac{-S}{2} \quad (6)$$

where  $S$  is the slope of the most suitable straight line, having the wavenumber,  $k$ , expressed in radians per kilometer. If, however, the frequency unit is expressed as cycles per kilometer, then the equivalent relation can be stated as

$$d = \frac{-S}{4\pi} \quad (7)$$

In estimating the depths from the power spectrum, the TMI grid is split into 49 overlapping blocks of 55 km  $\times$  55 km (Figure 5a). Many researchers believe that the window size should be at least four or six times the magnetic source depth being targeted [19,46,47]. This implies that some prior knowledge of the targeted magnetic sources is required for optimal window size selection. Previous geophysical studies using magnetic and gravity data in various parts of the Benue Trough [21,22,45,48] estimated basement depths ranging from 2 to 9 km.

Magnetic data can be reduced-to-pole (RTP) or reduced-to-equator (RTE) in order to center the anomaly peaks over the causative sources. However, at low magnetic latitude (less than 20° inclination), RTP correction is ineffective, particularly for north–south trending geologic features, due to extreme distortion of anomaly and unreasonable amplification of noise [8,40]. RTE is recommended as an alternative [49], but for this study, which is located near the Equator (less than 10° latitude), the RTE grid computed using a geomagnetic inclination of  $-8.0$  and declination of  $-1.7$  did not produce any significant improvement over the TMI grid. As a result, it is preferable to use the TMI rather than the RTE [45] and avoid all of the FFT processes involved in the RTE correction. To suppress the extremely shallow anomalies which are mostly noise, the TMI was continued upward for 0.8 km (Figure 5b) before applying the edge enhancement filters. However, because the noise will be at the tail of the spectrum, the spectral depth analysis was performed on the original TMI without the upward continuation.

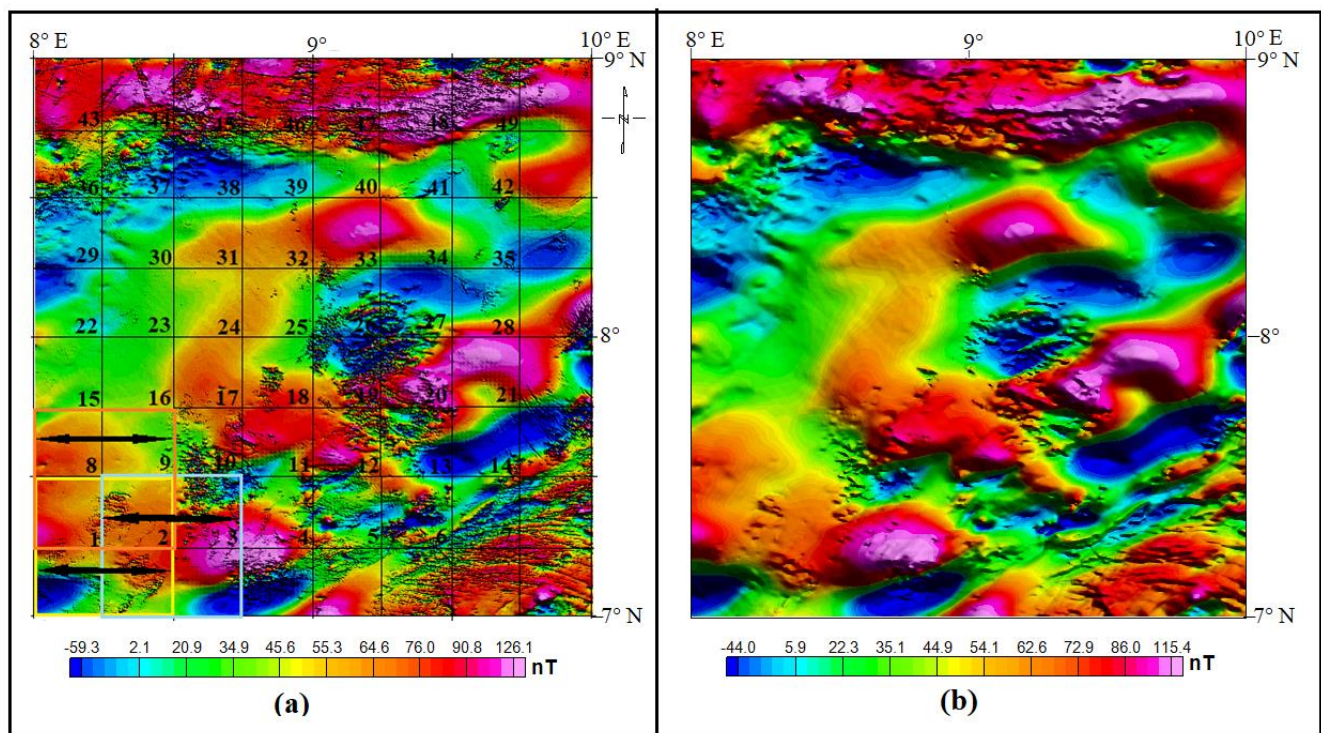


**Figure 5.** (a) The TMI map showing the division of the spectral blocks into 55 km × 55 km with 50% overlap. The block's centers are numbered from 1–49. The boundaries of blocks 1, 2, and 8 are shown by yellow, blue, and orange lines, respectively. (b) The upward-continued TMI map.

## 4. Results

### 4.1. Mapping of Intrusive and Volcanic Rocks (Intrasedimentary Features)

Application of digital filtering operations such as derivative analysis on magnetic data is an important tool in geological mapping since it improves the details on the map, particularly in places with limited or no bedrock exposures. The magnetic derivatives of the TMI data of the study area were utilized to map intrasedimentary volcanic rocks, as well as their spatial distribution within the Middle Benue Trough (MBT). The derivative analysis was also used to delineate the Basement Complex–sedimentary basin contact. Zoning of magnetic maps, according to Reeves [18], into different geological units based on a distinctive or well-defined anomaly pattern is an important part of qualitative interpretation. As a result, the resultant derivative maps were clearly delineated into different geological units. The regions of intense volcanic activities were demarcated into zones 1–3, while other areas of sporadic Tertiary volcanism and intrasedimentary intrusives were also delineated. The results of the various derivatives computed and utilized for the intrasedimentary and volcanics mapping are displayed in Figure 6a–d.

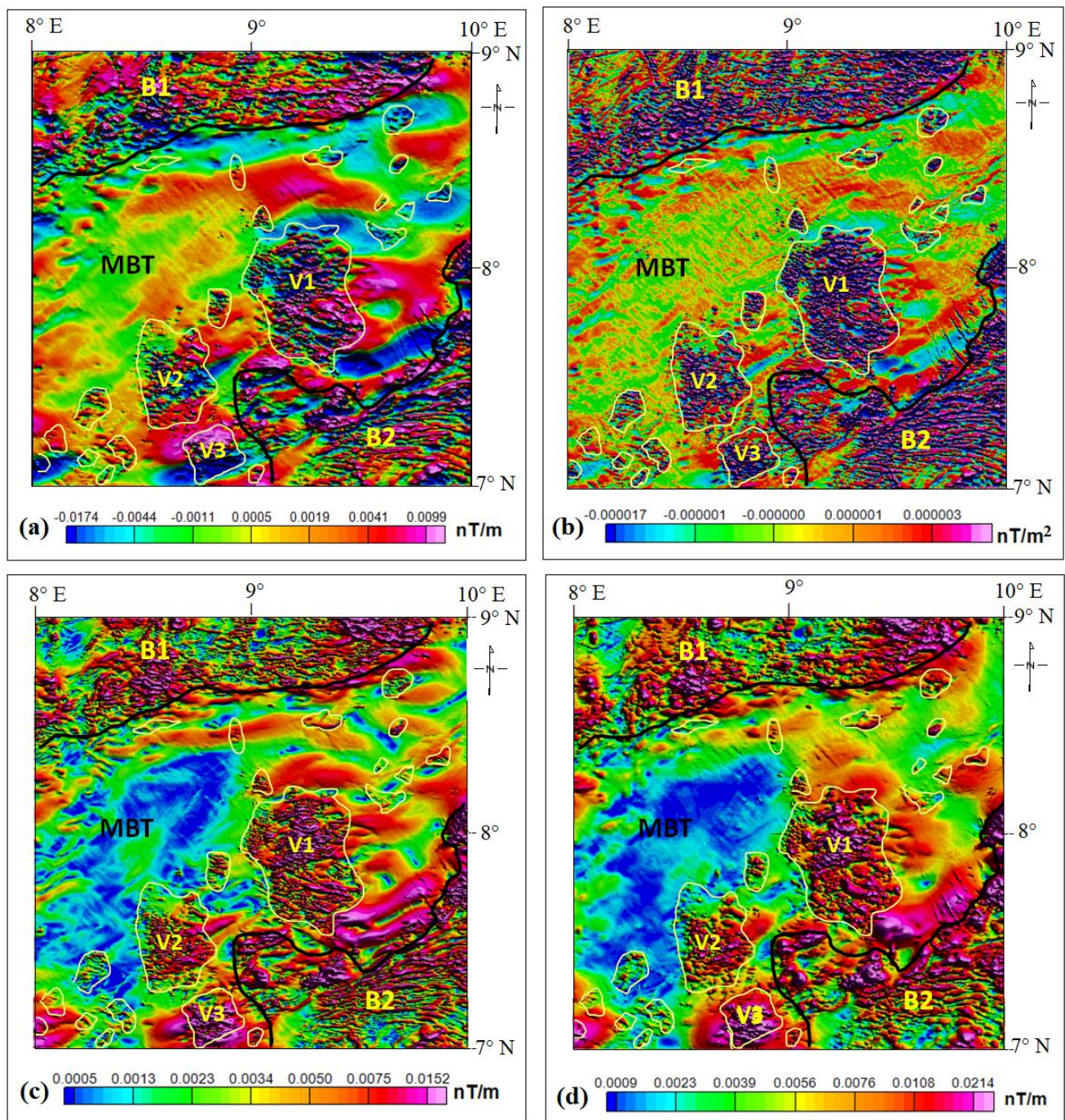


**Figure 6.** Magnetic derivatives maps of the study area depicting the sedimentary–basement contact, as well as volcanics and intrasedimentary features. (a) 1VD. (b) 2VD. (c) THDR. (d) AS.

Major structural and lithological details which are not effectively displayed in the TMI are efficiently enhanced in the 1VD map (Figure 6a). The 1VD map reveals a strong NE–SW structural lineation (long-wavelength anomalies) which is in alignment with the orientation of the Benue Trough, and other weaker lineation in NW–SE and E–W directions (short-wavelength anomalies). These identified trends can be attributed to the extensional

basin tectonics resulting in the creation of the Benue Trough. Further examination of the 1VD map reveals high density of fracturing in the Basement Complex region in the extreme northern and southern parts of the study area. Intense fracturing can also be observed in some central portions where the basement outcrops and in areas of near-surface intrusions. The 2VD operation is a more intense filter than the 1VD, hence shallow features such as near-surface faults and other lineaments that are not revealed by the 1VD can be observed here. The minutest of magnetic sources are captured even very close to the Earth's surface. From the 2VD map (Figure 6b), aggregate of isolated sources producing the anomalies can be observed. The THDR operation is effective in revealing boundaries of susceptibility contrast and serves as good edge detector by computing the maxima over the edges of structures (Figure 6c). The THDR map also reveals the lineation from the magnetic sources to be majorly in the NE–SW and NW–SE directions, while there are minor lineaments in the E–W and N–S directions. The AS map (Figure 6d) displays maximum value over magnetization contrasts as can be observed around the basement–sediment contact in the northern and the southeastern parts of the study area. In addition, volcanic intrusions with other intrasedimentary features are effectively displayed and delineated on the AS map, occurring mostly around the central portion. The TDR function is effective at detecting sources of both shallow and deeper depths; hence it is good in displaying overall lineaments both from shallow and deeper sources (Figure 7). The tilt derivative of the study area shows consistency in general orientations of lineaments derived from other derivatives.

Around the major volcanic zones delineated as V1–V3, the derivative maps show aggregates of isolated clusters of very short-wavelength anomalies, with other noticeable high-amplitude anomalies corresponding to known exposure or outcrops of intrasedimentary volcanics. Other high-amplitude, short-wavelength anomalies linked to the surface and near-surface intrasedimentary volcanics were greatly enhanced by these magnetic derivative maps generated through edge enhancement methods; thus, sporadic occurrences of volcanic rocks around the axis of the Middle Benue Trough were recognized and mapped. This derivative analysis demonstrates that the Late Cretaceous–Tertiary volcanism is far more extensive than the surface geological mapping suggests, extending across the axis of the Cretaceous MBT.

#### 4.2. Structural Delineation

The zero contour values depicting magnetic source edges on the first and second vertical derivative maps and the tilt derivative map, as well as the maxima/ridges on the total horizontal derivative map and the analytic signal map, were effectively utilized in the structural delineation of the region. Consequently, linear features with length of over 3 km were deemed structurally significant and designated as magnetic lineation and traced on the TDR map. Because the zero crossing of the TDR accurately delineates the edges of structures, it is considered a good enhancement operation in delineating basement faults [45]. The delineated faults from TDR were combined with data from other derivatives maps to create a regional structural map of the study area (Figure 8a). Because of their linear shape, the bulk of the magnetic lineaments mapped out are thought to be caused by faults, joints, contacts, and shear zones. Their length ranged from 3 km to more than 70 km, and those with linear extent of more than 20 km in length are assumed to be regionally significant and thus inferred as major faults. They are thought to be deep-seated faults associated with the Cretaceous rifting episode that gave birth to the MBT. The azimuths of these geologic structures/lineaments were measured and are displayed on a rose diagram (Figure 8b). The prevailing strike of these structures was observed to be in the NE–SW and NW–SE directions, with a few in the E–W trend.

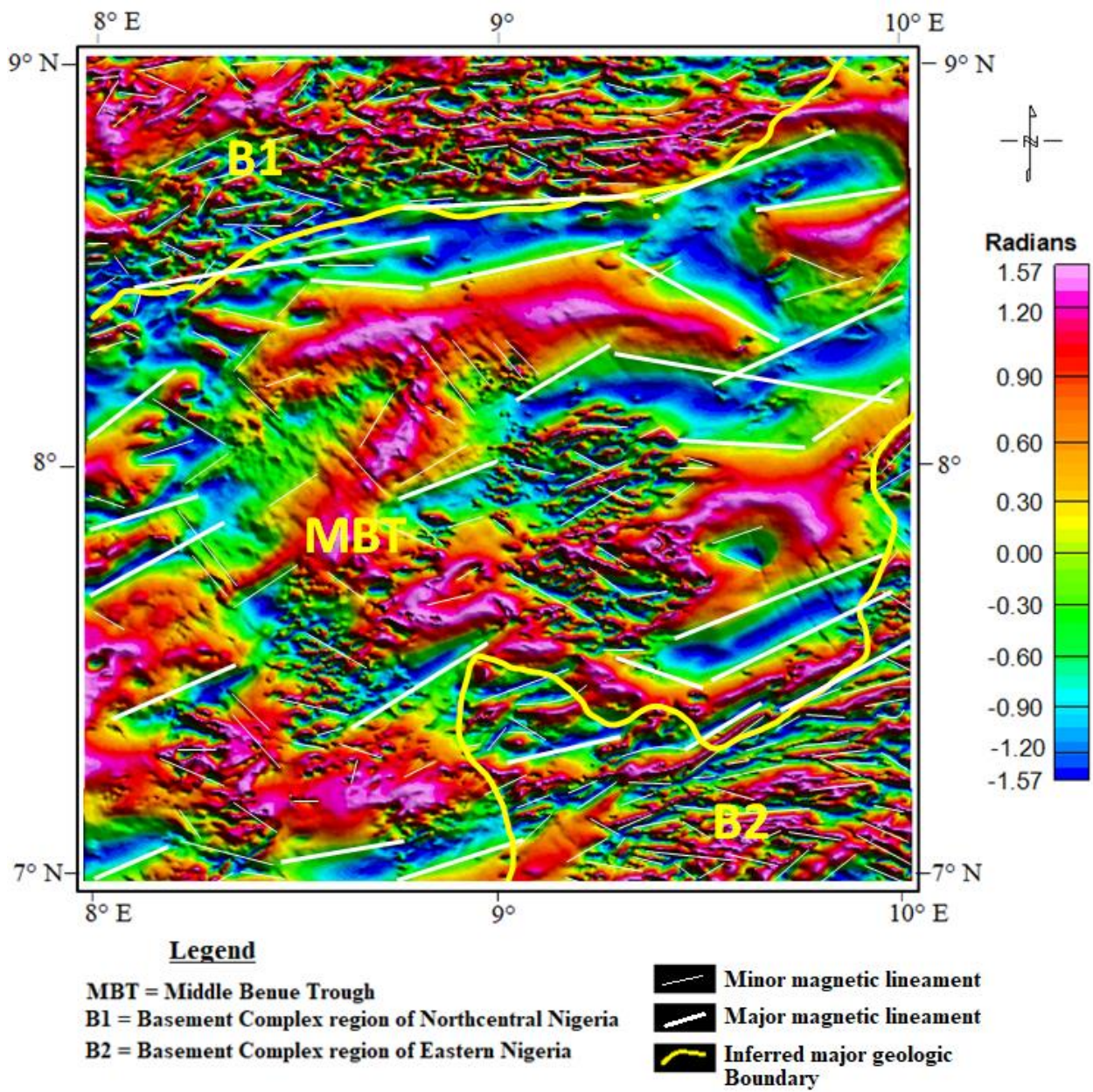
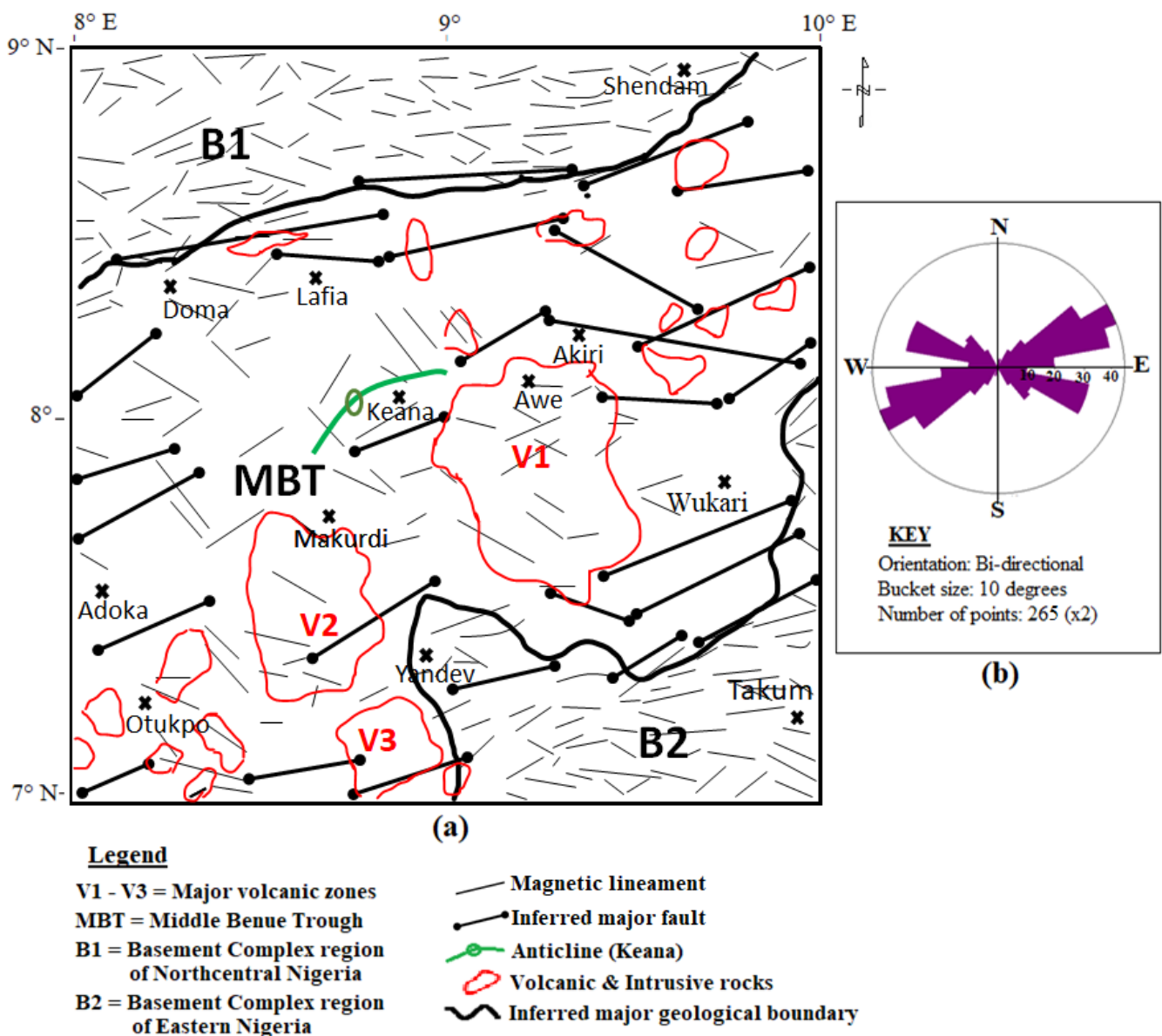


Figure 7. TDR map of the study area.



**Figure 8.** (a): Structural map obtained from magnetic derivatives of the area. (b): Rose diagram showing the orientation of the faults.

### 4.3. Results of Spectral Depth Analysis

The findings of the spectral depth analysis, presented in Figures 9 and 10, and Table 1, indicate the existence of two significant magnetic source depths for each block displayed in Figure 5a: the deeper depth (D1) and the shallower depth (D2). While the deeper depth is assumed to reflect the relief of the basement surfaces, the shallower depths, however, represent depths to top of intrusives and other intrasedimentary magnetic bodies. The deep magnetic source depth which ranges from 1.9–6.1 km, with an average of 3.9 km, is obtained from the low-frequency components of the spectrum and found to be undulating (Figure 11) and consisting of several horst and graben structures. These varying depths can be attributed to the influence of magnetic rocks invading onto the basement surface, lateral changes in basement susceptibilities, and features such as fractures and faults. The shallow magnetic sources, as defined by the higher frequency components of the spectrum, range from 0.3–1.9 km with an average of 0.8 km. These depths are signals from post-Cretaceous near-surface intrusions of magnetic bodies into overlying sediments, as well as signals emanating from ferruginized sandstones and ironstones occurring with the sediments.

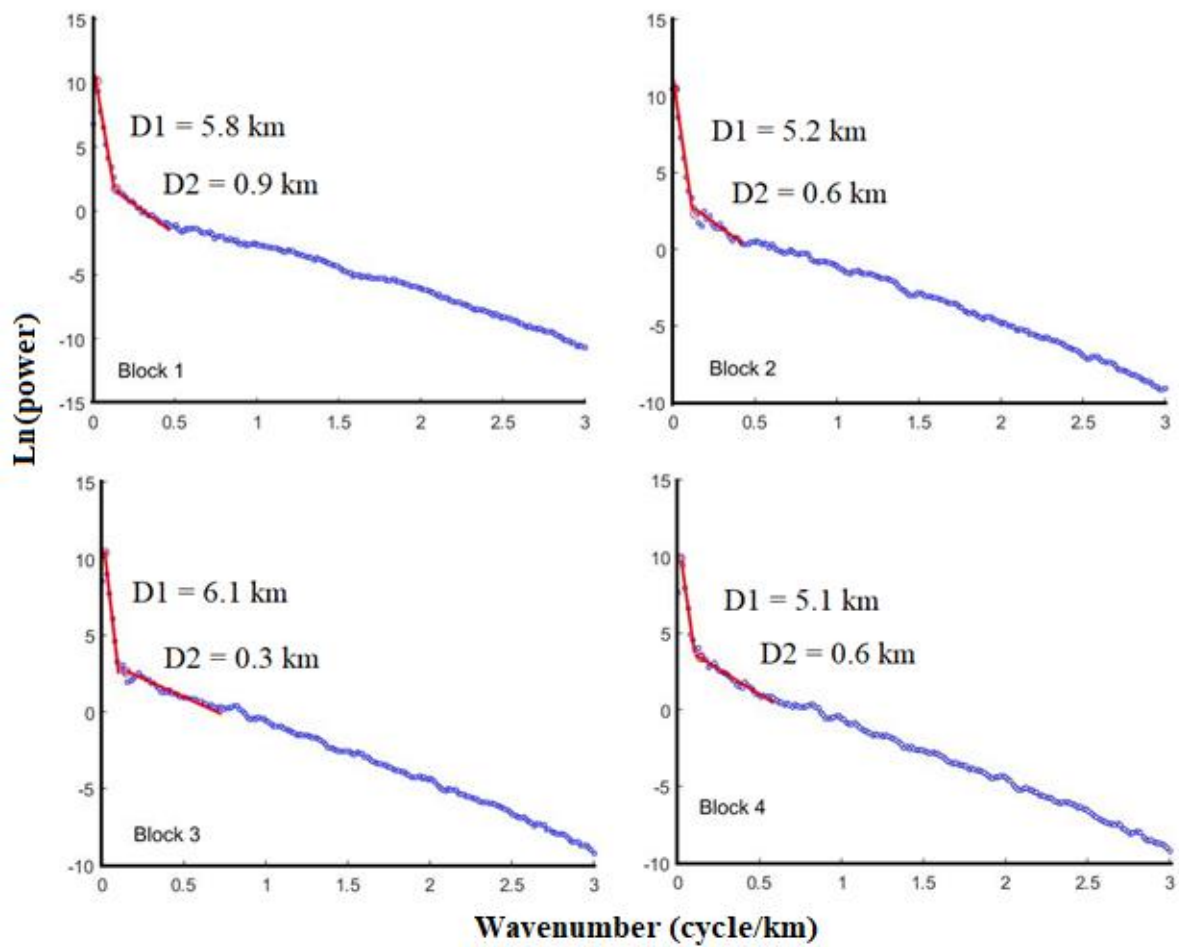


Figure 9. Plots for the power spectrum for blocks 1–4 (as displayed in Figure 5a). The depths to the deeper and shallower magnetic sources are represented by D1 and D2, respectively.

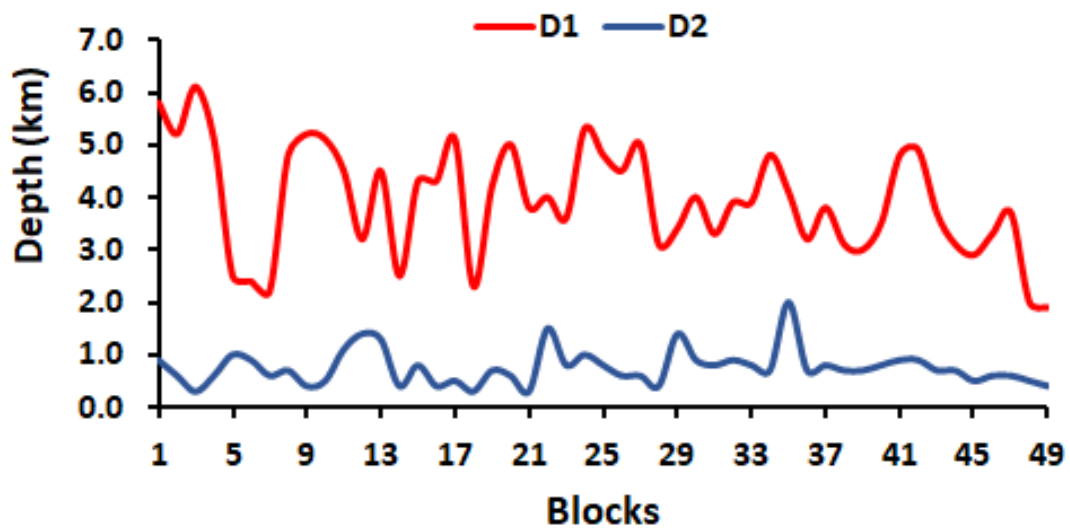
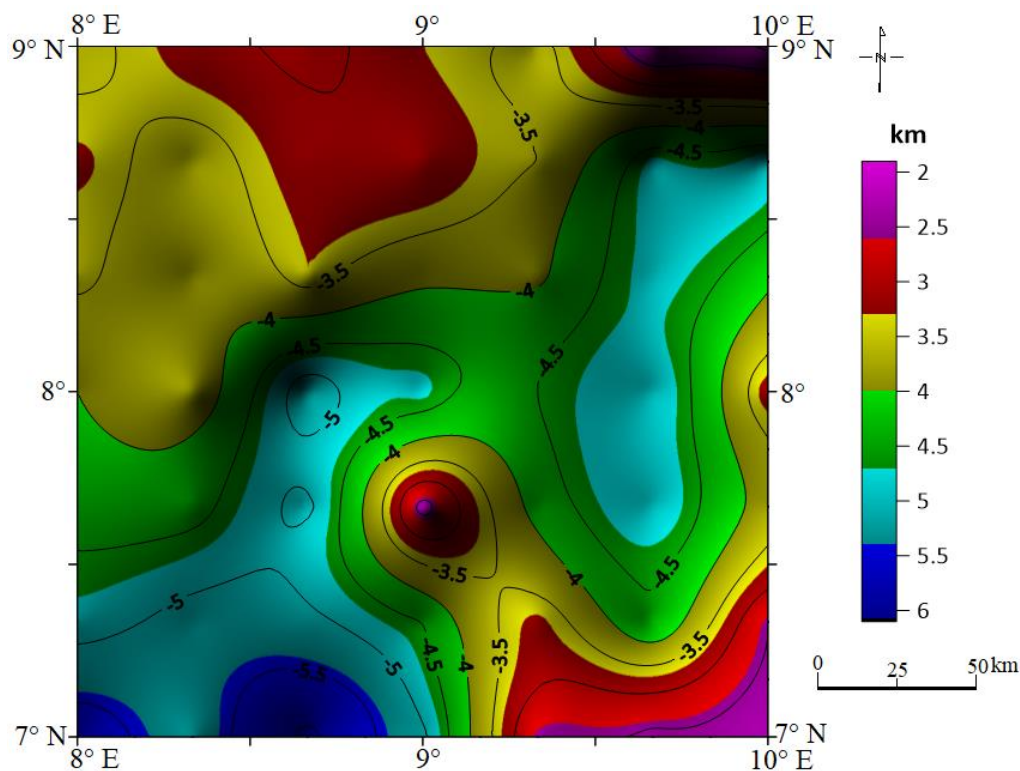


Figure 10. Depth variations across the study area, for the blocks displayed in Figure 5a. D1 and D2 represent deep and shallow depths to magnetic sources. The deeper depths are assumed to coincide with the top of the basement, while the shallower depths probably emanate from intrusives and other intrasedimentary sources.

**Table 1.** Results of the deeper (D1) and the shallower (D2) magnetic sources for the blocks displayed in Figure 5a.

Block	D1 (km)	D2 (km)	Block	D1 (km)	D2 (km)
1	5.8	0.9	26	4.5	0.6
2	5.2	0.6	27	5.0	0.6
3	6.1	0.3	28	3.1	0.4
4	5.1	0.6	29	3.4	1.4
5	2.5	1.0	30	4.0	0.9
6	2.4	0.9	31	3.3	0.8
7	2.2	0.6	32	3.9	0.9
8	4.8	0.7	33	3.9	0.8
9	5.2	0.4	34	4.8	0.7
10	5.1	0.5	35	4.1	2.0
11	4.5	1.1	36	3.2	0.7
12	3.2	1.4	37	3.8	0.8
13	4.5	1.3	38	3.1	0.7
14	2.5	0.4	39	3.0	0.7
15	4.3	0.8	40	3.5	0.8
16	4.3	0.4	41	4.8	0.9
17	5.1	0.5	42	4.9	0.9
18	2.3	0.3	43	3.7	0.7
19	4.2	0.7	44	3.1	0.7
20	5.0	0.6	45	2.9	0.5
21	3.8	0.3	46	3.3	0.6
22	4.0	1.5	47	3.7	0.6
23	3.6	0.8	48	2.0	0.5
24	5.3	1.0	49	1.9	0.4
25	4.8	0.8	-	-	-



**Figure 11.** Map of the area's deeper magnetic depth, which is assumed to coincide with the basement surface. The contours indicate depth from ground surface to the top of basement.

#### 4.4. Field Observations

The results of field observations carried out around this area reveal the presence of volcanic rocks (basalts) found in several outcrops within the MBT. One of such locations is on Azara–Wuse Road, with precise bearing of latitude  $8^{\circ}21'51''$  N and longitude  $9^{\circ}17'20''$  E, southwest of Akiri, where basaltic rocks were found intruding into the Cretaceous sandstone and siltstone of the Awe Formation (Figure 12a). Severe faulting and fracturing were also observed around the Awe hot spring. This is attributed to the numerous tectonic activities that have been documented in the region, especially during the rifting process of the Benue Trough in the Early Cretaceous and the folding and compressional activities in the Santonian [26,50]. These lineaments around the Awe hot spring trend dominantly in the NE–SW and NW–SE directions (Figure 12b). The MBT is noted for the occurrence of several hydrothermal mineral deposits such as salt, barite, lead–zinc, limestone, and gypsum, among others [24,51]. Salt and barite mineralization were observed to occur extensively in the area (Figure 12c,d). Around the Akiri hot spring, large deposits of salt were seen on the ground surface, which were likely precipitated from the groundwater as a result of the anomalous temperature of the area. In other locations, salts were also seen crystallizing out of the sandstones of the Keana Formation westwards from Akiri towards Keana. This salt mineralization could also have influenced the pH of the springs as well as the groundwater and other streams and rivers in the area. According to Lar and Sallau [51], the Keana and Awe areas, since time immemorial, have been known for their indigenous salt manufacturing and trading. As a result, salt has played a significant role as a domestic and industrial good in the region.



**Figure 12.** Structures and mineralization around the Akiri and Awe hot springs in the Middle Benue Trough. (A) Tertiary basalt intruding the Cretaceous sandstone of the Awe Formation. (B) Intense faulting and fracturing at the vicinity of the Awe hot spring due to heavy tectonic activities around the area, resulting in lineaments predominantly trending in NE–SW and NW–SE directions. (C) Salt (NaCl) mineralization around the Akiri hot spring. (D) Barite ( $\text{BaSO}_4$ ) mining at the MBT. Barium sulfate is formed in veins and fractures as a result of hydrothermal crystallization.

## 5. Discussion

### 5.1. Tectonism and Magmatism

Low-amplitude anomalies related to the Cretaceous sedimentary rocks of the Middle Benue Trough and high-amplitude anomalies linked to intrusive and volcanic rocks (intrasedimentary) are observable on the magnetic derivative maps (Figure 6). The derivatives also reveal high-amplitude anomalies over the area underlain by crystalline Basement Complex rocks on the northern and southeastern margins of the study area. The presence of several isolated aggregates of intrasedimentary volcanic rocks was also exposed and effectively delineated. Surface and near-surface/shallow geologic bodies such as volcanics/intrusives are predominantly responsible for high-frequency and short-wavelength anomalies, while deeper geologic bodies are primarily responsible for long-wavelength anomalies [1]. Vertical derivatives, in general, accentuate the edges of anomalies and improve the physical description of shallow causative geologic bodies. A noteworthy example may be found in the basin's central portion, where the vertical and horizontal derivatives, as well as the analytic signal, visibly established the outlines of the three major volcanic zones (V1, V2, and V3). The younger basalt (Neogene–Tertiary) and the older basalt (Paleogene volcanism) mapped out around Akiri and Awe, south of Makurdi, and southwest of Yandev in the geologic map published by the Nigeria Geological Survey Agency [33] (Figure 2), correlates well with the high-frequency and short-wavelength components delineated on the derivatives anomaly maps produced in this study. There was also substantial correlation with several of the Tertiary basalt surface exposures identified during the field observations. These include the aggregates of volcanic rocks (basalt) scattered between the southwest of the Akiri hot spring and northeast of the Awe hot spring, as well as the Tertiary basalt that intruded the sandstones of the Awe Formation in the Middle Benue Trough, about 3 km from the Akiri hot spring. Because the volcanic rocks are basic to intermediate in composition and, thus, dense, the presence of multiple near-surface intrasedimentary rocks observed in this study agrees with gravity results of Ajayi and Ajakaiye [48] suggesting that the Trough's central axis has a positive Bouguer anomaly, most likely due to basalt's relatively high density of  $2.9 \times 10^3 \text{ kg/m}^3$  recorded by them. The positive Bouguer anomaly reported around these major volcanic zones (V1–V3) could be attributable to basic intrusives with high magnetite concentrations. Basic volcanic rocks exhibit high magnetic susceptibility [52], which is most likely responsible for the high-amplitude/short-wavelength magnetic anomalies displayed by the zones. Since basic volcanic rocks are primarily mantle-derived, suggesting the presence of deep-seated fractures underneath the MBT which could have served as pathways for the upcoming mantle lava, accompanied by high heat flux into the sediments. These also are connected to the widespread intrasedimentary volcanic rocks in the region, linked to Tertiary magmatism, which most likely constituted the Benue Trough's second rifting episode [53], believed to have been facilitated by these deep-seated fractures. Since most mineralization occurs in places with widespread volcanic rocks and structures [1], the spatial distribution of various hydrothermal mineral deposits, for instance lead–zinc–barite mineralization, in the Trough is associated with magmatic processes and governed by pre-existing tectonic structures.

The presence of geologic structures trending predominantly NE–SW and NW–SE, as well as minor trends of E–W and N–S, suggests that the study area has undergone differential stress regimes in conjunction with multiple episodes of tectonic deformation across geologic time. In addition, these variations in structural alignment within the MBT could have resulted from crustal forces transferred via weaker sediments in orientations other than the underlying basement's primary tectonic trend. Some surface outcrops observed during the fieldwork exercise, as well as previous geophysical and remote sensing data [1,26,45,54], substantiate these multiple structural trends. The Benue Trough's alignment was most likely influenced by the NE–SW striking dextral shear zones of the Pan-African age [53,55]. The Romanche fracture zones, as well as the Chain and Charcot fracture zones associated with major plate tectonism in the South Atlantic, are believed to have continental extensions that have influenced the major NE–SW fracture system

along the Benue Trough through pre-existing lines of weakness, as reported by previous studies [31,56]. These pre-existing lines of weakness were most likely formed during the Pan-African orogeny but became active in the Cretaceous during the opening of the South Atlantic, resulting in a rejuvenation of the continent's fault system. As a result, Cratchley et al. [31] suggest a transcurrent movement pattern, with the Benue Trough possibly representing the continent's extension. This dominant alignment is also probably connected to the ductile shear fault zones in the Potiguar Basin of the NE Brazilian rift system, thought to be the equivalent of the Benue Trough, and reported to exhibit similar deep-seated basement structural orientation, according to de Castro et al. [57]. As a result, the NE–SW trending Neoproterozoic–Early Paleozoic ductile shear zones are linked to deep-seated basement tectonic structures that likely played a key role in the evolution of the Benue Trough, whereas the Late Jurassic–Early Cretaceous reactivation of ancient sinistral shear zones, transtensional, and transpressional tectonics may have shaped the basement configuration underneath the Trough, and, ultimately, its orientation and layout. Consequently, most of the significant tectonic structures trending in the NE–SW direction, according to Ajakaiye et al. [58], could be inferred as strike-slip faults probably linked with transcurrent movements in a similar direction. While the NE–SW major trend is of regional significance that transcends beyond the shores of the African continent, the NW–SE trends, however, are more confined and associated with the Bida Basin in North Central Nigeria, Yola Arm of the Benue Trough in Northeast Nigeria, Garoua Trough in Cameroon, and other West and Central African Rift Systems (Figure 1). Compressional events, particularly in the Santonian, which probably reactivated pre-existing shear zones in the Benue Trough [26], must have resulted in the formation of the majority of the N–S and E–W trends, as well as some NW–SE lineation observed within the trough. These faults are associated with the folding episodes that generated the Benue Trough's great folds, such as the Keana anticline in the MBT (Figure 8a), the Abakaliki anticlinorium in the LBT, and the Lamurde anticline in the UBT [45], and may be related to deep-seated movements in the underlying basement. According to Wright [29], most of the major folds in the Benue Trough are probably drape folds manifested in the overlying sediments, caused by differential uplift of the basement faulted blocks. This is based on evidence from the Lamurde anticline in the UBT having straight limbs that trend in the NE–SW direction, and shown by Ogunmola et al. [45], from aeromagnetic and satellite data, to likely be an expression of massive basement faults.

Hydrothermal mineral occurrences within the Middle Benue Trough are quite extensive and their deposits include barite, lead–zinc, limestone, gypsum, and a variety of others. These mineral deposits are concentrated around various portions of the MBT, especially where the Tertiary volcanism is observed to have been the most intense. The majority of these mineralized zones occur as veins, faults, and fractures mostly trending in the NW–SE direction [51,59]. This indicates that the Santonian compressional tectonic events which resulted in the formation of several folds and anticlinal structures, as well as several younger fractures, must have created the host sites for the mineralization. Subsequently, the Cenozoic magmatism must have aided in the hydrothermal alteration processes and remobilization of these minerals into the pre-existing lines of weakness. The salt mineralization, sometimes referred to as brine, is mostly made up of  $\text{Na}^+$  and  $\text{Cl}^-$  salts; however, evidence of metal radicals such as Ba, K, Mg, Mn, Li, and Ca have been detected in the brines [51]. Although this salt mineralization occurs extensively in the axial portion of the Keana anticlinorium, the entire area from Keana down to Akiri and Awe, in the middle portion of the study area around volcanic zone 1 (V1), is observed as having the highest concentration of these salt deposits, and was referred to as Awe and Keana brine fields by Offodile [60], and Lar and Sallau [51], respectively. The salt's origin is still unclear, as different researchers have brought forth different hypotheses. For instance, Uma [61] opined that perhaps most of the brine existed before the magmatic activities, implying that the brines might have been deposited with the Mid-Cretaceous sediments before tectonic activities, resulting in sediment compaction, folding, and fracturing, accompanied by mag-

matic activities, thus resulting in hydrothermal upsurge and, subsequently, the expulsion of saline interstitial water into fracture spaces. Offodile [60], however, suggested that while the tectonics around the area indicate the possibility of salt dome features, it could also be that evaporites might have been deposited along with the Asu River Group and Awe Formation depositional cycle during the marine transgression and regression phases of the Albian to the Cenomanian periods. Nonetheless, the high volcanic activities with the consequent high heat flow might have facilitated the precipitation of these salt crystals in the area. In general, it is believed that the widespread occurrence of hydrothermal mineral deposits is an indicator of the area's substantial tectonic and volcanic imprints.

## 5.2. Depth Delineations

The spectra depth analysis revealed a two-source depth model cutting across diverse lithological units within the MBT. The deep depth, which is assumed to coincide with the basement, ranges from 1.9–6.1 km, while the shallow depth, comprising younger intrusives and other magnetic near-surface bodies, ranges from 0.3 to 1.9 km. The Basement Complex region of Central, as well as Eastern, Nigeria encroached into the study area from the northern and the southeastern margins of the Middle Benue Trough, respectively. These areas are typically made up of crystalline rock units but hosting sediments up to 3.5 km thick, which progressively become thinner away from the basin. Around the southeast region, the basement is uplifted with depth ranges of about 2 km, and geologically belongs to the Migmatite Gneiss Complex of the Eastern Nigerian Basement. The rock unit in this area consists mostly of banded gneiss with older granite (Pan-African granitoids), believed to be Precambrian in age [24]. The basement depths in the northern borders range from 1.9 to 3.5 km and correspond to the migmatite zone of the Central Nigerian Basement Complex, comprising rock units of migmatite, gneiss, and Older Granites. Based on observations of the basement floor and the faulted structures surrounding the Keana anticline, the surface expression of the anticlinoria may be a manifestation of differential uplift in basement faulted blocks, which could have resulted in a drape fold. Underneath the fold limbs, there could be traps for mineralization, which needs to be further investigated in subsequent research. The analysis also yielded great basement depths ranging from 4–6.1 km which correspond to different parts of the graben basin. These are the deepest areas of the subsided underlying basement surfaces, which are filled with thick Cretaceous sediments. Overall, the results of the basement surface delineation indicate that the surface expression of the basement underneath the MBT is quite irregular, depicting series of horst and graben structurally controlled sub-basins, which most likely were formed from displacements of several faulted basement blocks during the rifting episode in the Cretaceous. Gravity studies, according to Ajakaiye [62], have revealed the existence of multiple basinal structures in the Benue Trough that are filled with Cretaceous sediments of varied thickness, which is consistent with the findings of this study.

The shallow magnetic depths (D2), which range from 0.3 to 1.9 km, are depths emanating from magnetic signals of post-Cretaceous near-surface intrusions as well as other magnetized bodies, such as ferruginized sandstones and ironstones embedded within the sediments. Igneous intrusion processes are phenomena usually associated with tectonic events of most rifted basins worldwide. Magmatism underneath the Benue Trough and its imprints appeared to have an impact on practically all basement surfaces. The intrusives in the MBT can be classified into two categories: the younger and older intrusives. The older intrusives are Pan-African in age ( $\geq 600$  Ma), comprising mostly granites, and are generally referred to as the Older Granites or Pan-African granitoids. They are not really considered, in most cases, as intrusives because of their age and association with the basement surfaces. However, zones of the older granites in the south around Yandev and in the north around Garaku yielded deep magnetic depths of about 3.5 km and shallow magnetic depth of between 0.7–1 km. The wide variation in depth around these older granitic zones is most likely related to their mode of formation. Most of the Older Granites were intruded during the evolution of gneisses and migmatites to form the Basement Complex together [63], and

occasionally protrude into overlying sediments as intrusions, with varying amounts of recrystallisation and depths of emplacement. The younger intrusives, with age ranging from Tertiary–recent, found within the MBT and the adjoining Basement Complex regions, are primarily granitic and pegmatitic, with sporadic occurrences of diorites, dolerites, and syenites, and a plethora of associated dyke-like bodies ranging in size from minor to massive [35]. The major volcanic zones (V1–V3) yielded shallow magnetic depths ranging from 0.3 to 0.6 km, indicating that the active magmatism of those zones might have influenced the depth of the emplacements.

## 6. Conclusions

Structural assessments as well as intrasedimentary volcanics and the depths to magnetic sources were delineated within the Middle Benue Trough. The variable deep magnetic depths (D1) as well as the shallow depths (D2), ranging from 0.3 to 6.1 km obtained, together with the structural evaluations, indicate that the basement surface is undulating and heavily faulted, forming some horst and graben structures, with presence of multiple magmatic intrusions into the Cretaceous sediments. Some of these fault planes, especially those trending in the NE–SW direction, have regional significance related to the rifting of the Benue Trough.

In conclusion, some of the major highlights of this study are as follows:

(1) The imprints of the Cenozoic volcanism and plutonism in the MBT are more extensive than contained in most published geological maps.

(2) Major basement faults with other aggregates of minor faults in the area may have served as pathways for heat transfer, which could have facilitated the hydrothermal mineralization in the MBT.

(3) The Keana anticline may be a manifestation of differential uplift in dip-slip basement faulted blocks which could have resulted in a drape fold, similar to the Lamurde anticlinorium in Upper Benue Trough, as suggested by Wright [56] and Ogunmola et al. [45], as opposed to the strike-slip model proposed by Ajayi and Ajakaiye [50].

(4) With the sediment thickness up to 6 km, as well as widespread occurrences of volcanism and plutonism resulting in high heat flow in the MBT, its suitability for hydrocarbon generation should be of interest to petroleum explorations in terms of enhanced maturation of petroleum source rocks.

**Author Contributions:** Conceptualization, E.G.E.; methodology, E.G.E. and N.E.H.I.; software, E.G.E.; validation, E.G.E., N.E.H.I., and I.Y.; formal analysis, E.G.E.; investigation, E.G.E.; resources, N.E.H.I. and I.Y.; data curation, E.G.E., N.E.H.I., and I.Y.; writing—original draft preparation, E.G.E.; writing—review and editing, E.G.E., N.E.H.I., and I.Y.; visualization, N.E.H.I. and I.Y.; supervision, N.E.H.I. and I.Y.; project administration, N.E.H.I. and I.Y.; funding acquisition, E.G.E. and N.E.H.I. All authors have read and agreed to the published version of the manuscript.

**Funding:** This research received no external funding.

**Data Availability Statement:** Data presented in this study are available on request from the corresponding authors.

**Acknowledgments:** The authors wish to acknowledge the Nigerian Geological Survey Agency (NGSA) for providing the aeromagnetic data. In addition, many thanks to the editors and the four anonymous reviewers for their efforts in improving the quality of the manuscript.

**Conflicts of Interest:** The authors declare no conflict of interest.

## References

1. Anudu, G.K.; Stephenson, R.A.; Macdonald, D.I.M. Using high-resolution aeromagnetic data to recognise and map intra-sedimentary volcanic rocks and geological structures across the Cretaceous middle Benue Trough, Nigeria. *J. Afr. Earth Sci.* **2014**, *99*, 625–636. [[CrossRef](#)]
2. Ekwok, S.E.; Akpan, A.E.; Achadu, O.-I.M.; Eze, O.E. Structural and lithological interpretation of aero-geophysical data in parts of the Lower Benue Trough and Obudu Plateau, Southeast Nigeria. *Adv. Space Res.* **2021**, *68*, 2841–2854. [[CrossRef](#)]

3. Ejiga, G.E.; Yusoff, I.; Ismail, N.E.H.; Usman, U.A. Utilizing the Magnetic Source Edge Detection (MSED) method in mapping geologic features within a sedimentary basin. In National Geoscience Conference (NGC2019), Sabah, Malaysia. *War. Geol.* **2019**, *45*, 358–360.
4. Cordell, L.; Grauch, V.J.S. Mapping basement magnetization zones from aeromagnetic data in the San Juan basin, New Mexico. In *The Utility of Regional Gravity and Magnetic Anomaly Maps*; Hinze, W.J., Ed.; Society of Exploration Geophysicists: Tulsa, OK, USA, 1985; pp. 181–197.
5. Miller, H.G.; Singh, V. Potential field tilt—A new concept for location of potential field sources. *J. Appl. Geophys.* **1994**, *32*, 213–217. [[CrossRef](#)]
6. Roest, W.R.; Verhoef, J.; Pilkington, M. Magnetic interpretation using the 3-D analytic signal. *Geophysics* **1992**, *57*, 116–125. [[CrossRef](#)]
7. Verduzco, B.; Fairhead, J.D.; Green, C.M.; MacKenzie, C. New insights into magnetic derivatives for structural mapping. *Lead. Edge* **2004**, *23*, 116–119. [[CrossRef](#)]
8. Wijns, C.; Perez, C.; Kowalczyk, P. Theta map: Edge detection in magnetic data. *Geophysics* **2005**, *70*, L39–L43. [[CrossRef](#)]
9. Pham, L.T.; Van Vu, T.; Le Thi, S.; Trinh, P.T. Enhancement of potential field source boundaries using an improved logistic filter. *Pure Appl. Geophys.* **2020**, *177*, 5237–5249. [[CrossRef](#)]
10. Pham, L.T.; Eldosouky, A.M.; Oksum, E.; Saada, S.A. A new high resolution filter for source edge detection of potential field data. *Geocarto Int.* **2020**, 1–18. [[CrossRef](#)]
11. Nelson, J.B. Calculation of the magnetic gradient tensor from total field gradient measurements and its application to geophysical interpretation. *Geophysics* **1988**, *53*, 957–966. [[CrossRef](#)]
12. Christensen, A.N.; Dransfield, M.H. Airborne vector magnetometry over banded iron-formations. In *SEG Technical Program Expanded Abstracts 2002*; Society of Exploration Geophysicists: Houston, TX, USA, 2002; pp. 13–16.
13. Zhang, J.; Zeng, Z.; Zhao, X.; Li, J.; Zhou, Y.; Gong, M. Deep Mineral Exploration of the Jinchuan Cu-Ni Sulfide Deposit Based on Aeromagnetic, Gravity, and CSAMT Methods. *Minerals* **2020**, *10*, 168. [[CrossRef](#)]
14. Shebl, A.; Abdellatif, M.; Elkhateeb, S.O.; Csámer, Á. Multisource Data Analysis for Gold Potentiality Mapping of Atalla Area and Its Environs, Central Eastern Desert, Egypt. *Minerals* **2021**, *11*, 641. [[CrossRef](#)]
15. Oruç, B. Edge detection and depth estimation using a tilt angle map from gravity gradient data of the Kozaklı-Central Anatolia region, Turkey. *Pure Appl. Geophys.* **2011**, *168*, 1769–1780. [[CrossRef](#)]
16. Arisoy, M.; Dikmen, Ü. Edge detection of magnetic sources using enhanced total horizontal derivative of the Tilt angle. *Bull. Earth Sci. Appl. Res. Cent. Hacet. Univ.* **2013**, *34*, 73–82.
17. Ibraheem, I.M.; Haggag, M.; Tezkan, B. Edge Detectors as Structural Imaging Tools Using Aeromagnetic Data: A Case Study of Sohag Area, Egypt. *Geosciences* **2019**, *9*, 211. [[CrossRef](#)]
18. Reeves, C. *Aeromagnetic Surveys; Principles, Practice & Interpretation 2005*; Geosoft: Singapore, 2005; Available online: [www.geosoft.com](http://www.geosoft.com) (accessed on 10 December 2019).
19. Kumar, R.; Bansal, A.R.; Ghods, A. Estimation of Depth to Bottom of Magnetic Sources Using Spectral Methods: Application on Iran’s Aeromagnetic Data. *J. Geophys. Res. Solid Earth* **2020**, *125*, e2019JB018119. [[CrossRef](#)]
20. Spector, A.; Grant, F.S. Statistical models for interpreting aeromagnetic data. *Geophysics* **1970**, *35*, 293–302. [[CrossRef](#)]
21. Abdullahi, M.; Kumar, R.; Singh, U.K. Magnetic basement depth from high-resolution aeromagnetic data of parts of lower and middle Benue Trough (Nigeria) using scaling spectral method. *J. Afr. Earth Sci.* **2019**, *150*, 337–345. [[CrossRef](#)]
22. Ekwok, S.E.; Akpan, A.E.; Ebong, E.D.; Eze, O.E. Assessment of depth to magnetic sources using high resolution aeromagnetic data of some parts of the Lower Benue Trough and adjoining areas, Southeast Nigeria. *Adv. Space Res.* **2021**, *67*, 2104–2119. [[CrossRef](#)]
23. Kumar, R.; Bansal, A.R.; Anand, S.P.; Rao, V.K.; Singh, U.K. Mapping of magnetic basement in Central India from aeromagnetic data for scaling geology. *Geophys. Prospect.* **2018**, *66*, 226–239. [[CrossRef](#)]
24. Obaje, N.G. Geology and Mineral Resources of Nigeria. In *Geology and Mineral Resources of Nigeria*; Springer: Heidelberg, Germany, 2009; pp. 1–221.
25. Fairhead, J.D.; Binks, R.M. Differential opening of the Central and South Atlantic Oceans and the opening of the West African rift system. *Tectonophysics* **1991**, *187*, 191–203. [[CrossRef](#)]
26. Benkhelil, J. The origin and evolution of the Cretaceous Benue Trough (Nigeria). *J. Afr. Earth Sci. (Middle East)* **1989**, *8*, 251–282. [[CrossRef](#)]
27. Burke, K.C.; Whiteman, A.J. Uplift rifting and the breakup of Africa. In *Implications of Continental Drift to the Earth Sciences*; Tarling, D.H., Runcon, S.K., Eds.; Academic Press: London, UK, 1973; pp. 735–755.
28. Burke, K.; Dessauvagie, T.; Whiteman, A. Geological history of the Benue valley and adjacent areas. *Afr. Geol.* **1972**, *1*, 187–206.
29. Wright, J.B. Origins of the Benue Trough; A Critical Review. In *Geology of Nigeria*; Kogbe, C.A., Ed.; Elizabethan Press: Lagos, Nigeria, 1976; pp. 309–317.
30. Grant, N.K. South Atlantic, Benue Trough, and Gulf of Guinea Cretaceous Triple Junction. *Geol. Soc. Am. Bull.* **1971**, *82*, 2295–2298. [[CrossRef](#)]
31. Cratchley, C.R.; Louis, P.; Ajakaiye, D.E. Geophysical and geological evidence for the Benue-Chad Basin Cretaceous rift valley system and its tectonic implications. *J. Afr. Earth Sci.* **1984**, *2*, 141–150. [[CrossRef](#)]
32. Schull, T.J. Rift basins of interior Sudan: Petroleum exploration and discovery. *AAPG Bull.* **1988**, *72*, 1128–1142.

33. Nigeria Geological Survey Agency (NGSA). *Geologic Map of Nigeria*; Authority of Federal Republic of Nigeria: Abuja, Nigeria, 2011.
34. Offodile, M.E. *The Geology of the Middle Benue, Nigeria*; Paleontological Institute, University Uppsala: Uppsala, Sweden, 1976; Volume 4, pp. 1–166.
35. Ofoegbu, C.O. A review of the geology of the Benue Trough, Nigeria. *J. Afr. Earth Sci. (1983)* **1985**, *3*, 283–291. [[CrossRef](#)]
36. Seequent, L. Putting Nigeria on the Map. 2010. Available online: <https://www.seequent.com/putting-nigeria-on-the-map/> (accessed on 5 February 2021).
37. Paine, J.W. A comparison of methods for approximating the vertical gradient of one-dimensional magnetic field data. *Geophysics* **1986**, *51*, 1725–1735. [[CrossRef](#)]
38. Oruç, B.; Keskinsezer, A. Structural setting of the northeastern Biga Peninsula (Turkey) from tilt derivatives of gravity gradient tensors and magnitude of horizontal gravity components. *Pure Appl. Geophys.* **2008**, *165*, 1913–1927. [[CrossRef](#)]
39. Phillips, J.D. *Processing and Interpretation of Aeromagnetic Data for the Santa Cruz Basin-Patagonia Mountains Area, South-Central Arizona*; US Department of the Interior, US Geological Survey: Washington, DC, USA, 2002.
40. MacLeod, I.N.; Jones, K.; Dai, T.F. 3-D analytic signal in the interpretation of total magnetic field data at low magnetic latitudes. *Explor. Geophys.* **1993**, *24*, 679–688. [[CrossRef](#)]
41. Nabighian, M.N. The analytic signal of two-dimensional magnetic bodies with polygonal cross-section: Its properties and use for automated anomaly interpretation. *Geophysics* **1972**, *37*, 507–517. [[CrossRef](#)]
42. Li, X. Understanding 3D analytic signal amplitude. *Geophysics* **2006**, *71*, L13–L16. [[CrossRef](#)]
43. Hahn, A.; Kind, E.G.; Mishra, D.C. Depth estimation of magnetic sources by means of Fourier amplitude spectra. *Geophys. Prospect.* **1976**, *24*, 287–306. [[CrossRef](#)]
44. Negi, J.G.; Agrawal, P.K.; Rao, K.N.N. Three-dimensional model of the Koyna area of Maharashtra State (India) based on the spectral analysis of aeromagnetic data. *Geophysic* **1983**, *48*, 964–974. [[CrossRef](#)]
45. Ogunmola, J.K.; Ayolabi, E.A.; Olobaniyi, S.B. Structural-depth analysis of the Yola Arm of the Upper Benue Trough of Nigeria using high resolution aeromagnetic data. *J. Afr. Earth Sci.* **2016**, *124*, 32–43. [[CrossRef](#)]
46. Blakely, R.J. *Potential Theory in Gravity and Magnetic Applications*; Cambridge University Press: Cambridge, UK, 1996.
47. Nwogbo, P.O. Spectral prediction of magnetic source depths from simple numerical models. *Comput. Geosci.* **1998**, *24*, 847–852. [[CrossRef](#)]
48. Ajayi, C.O.; Ajakaiye, D.E. The origin and peculiarities of the Nigerian Benue Trough: Another look from recent gravity data obtained from the Middle Benue. *Tectonophysics* **1981**, *80*, 285–303. [[CrossRef](#)]
49. Leu, L.-K. Use of reduction-to-the-equator process for magnetic data interpretation. In *Geophysics*; Soc Exploration Geophysicists: Tulsa, OK, USA, 1982.
50. Ajayi, C.O.; Ajakaiye, D.E. Structures deduced from gravity data in the Middle Benue, Nigeria. *J. Afr. Earth Sci. (1983)* **1986**, *5*, 359–369. [[CrossRef](#)]
51. Lar, U.A.; Sallau, A.K. Trace element geochemistry of the Keana brines field, middle Benue trough, Nigeria. *Environ. Geochem. Health* **2005**, *27*, 331–339. [[CrossRef](#)] [[PubMed](#)]
52. Kearey, P.; Brooks, M.; Hill, I. *An Introduction to Geophysical Exploration*, 3rd ed.; Blackwell Scientific Publication: Oxford, UK, 2002.
53. Guiraud, R.; Maurin, J.-C. Early Cretaceous rifts of Western and Central Africa: An overview. *Tectonophysics* **1992**, *213*, 153–168. [[CrossRef](#)]
54. Ogunmola, J.K.; Gajere, E.N.; Ayolabi, E.A.; Olobaniyi, S.B.; Jeb, D.N.; Agene, I.J. Structural study of Wamba and Environs, north-central Nigeria using aeromagnetic data and NigeriaSat-X image. *J. Afr. Earth Sci.* **2015**, *111*, 307–321. [[CrossRef](#)]
55. Maurin, J.C.; Benkhelil, J.; Robineau, B. Fault rocks of the Kaltungo lineament, NE Nigeria, and their relationship with Benue Trough tectonics. *J. Geol. Soc.* **1986**, *143*, 587–599. [[CrossRef](#)]
56. Wright, J.B. Fracture systems in Nigeria and initiation of fracture zones in the South Atlantic. *Tectonophysics* **1976**, *34*, 43–47. [[CrossRef](#)]
57. de Castro, D.L.; Bezerra, F.H.R.; Sousa, M.O.L.; Fuck, R.A. Influence of Neoproterozoic tectonic fabric on the origin of the Potiguar Basin, northeastern Brazil and its links with West Africa based on gravity and magnetic data. *J. Geodyn.* **2012**, *54*, 29–42. [[CrossRef](#)]
58. Ajakaiye, D.E.; Hall, D.H.; Ashiekaa, J.A.; Udensi, E.E. Magnetic anomalies in the Nigerian continental mass based on aeromagnetic surveys. *Tectonophysics* **1991**, *192*, 211–230. [[CrossRef](#)]
59. Ford, S.O. The Economic Mineral Resources of the Benue through. *Earth Evol. Sci. Springer Nat.* **1981**, *2*, 154–163.
60. Offodile, M.E. The geology and tectonics of Awe brine field. *J. Afr. Earth Sci. (1983)* **1984**, *2*, 191–202. [[CrossRef](#)]
61. Uma, K.O. The brine fields of the Benue Trough, Nigeria: A comparative study of geomorphic, tectonic and hydrochemical properties. *J. Afr. Earth Sci.* **1998**, *26*, 261–275. [[CrossRef](#)]
62. Ajakaiye, D.E. Geophysical investigations in the Benue Trough—A review. *Earth Evol. Sci.* **1981**, *2*, 126–136.
63. Oyawoye, M.O. The Basement complex of Nigeria. In *African Geology*; Dessauvague, T.F.J., Whiteman, A.J., Eds.; Ibadan University Press: Ibadan, Nigeria, 1972; pp. 67–99.